

Preparation of PtSn/C and PtSnNi/C electrocatalysts using the alcohol-reduction process

Estevam V. Spinacé*, Luciana A. Farias, Marcelo Linardi, Almir Oliveira Neto*

Instituto de Pesquisas Energéticas e Nucleares - IPEN/CNEN-SP, Av. Prof. Lineu Prestes, 2242, Cidade Universitária, 05508-900, São Paulo-SP, Brazil

Received 26 May 2006; accepted 12 November 2007

Available online 17 November 2007

Abstract

PtSn/C electrocatalyst with Pt:Sn molar ratio of 50:50 and PtSnNi/C electrocatalyst with a Pt:Sn:Ni molar ratio of 50:40:10 were prepared by the alcohol-reduction process using ethylene glycol as solvent and reducing agent. The electrocatalysts were characterized by EDX, XRD, TEM and cyclic voltammetry. The electro-oxidation of ethylene glycol was studied by cyclic voltammetry and chronoamperometry using the thin porous coating technique. PtSnNi/C electrocatalyst showed a superior performance compared to PtSn/C electrocatalysts in the potential range of interest for direct ethylene glycol fuel cell.

© 2007 Elsevier B.V. All rights reserved.

Keywords: PtSn/C; PtSnNi/C; Alcohol-reduction process; Electro-oxidation; Ethylene glycol; Fuel cell

1. Introduction

A Direct Alcohol Fuel Cell (DAFC) is a device in which the alcohol is fed directly into the fuel cell without any previous chemical modification and is oxidized at the anode while oxygen is reduced to water at the cathode. Thus, DAFC are very attractive as power sources for mobile and portable applications because it is not necessary to convert the fuel in a reformer into hydrogen. However, alcohols are very difficult to electro-oxidize completely and up to now methanol has been considered the most promising organic fuel because it is more efficiently oxidized than other alcohols. On the other hand, it is toxic and the methanol crossover through the polymer–electrolyte membrane results in a decrease of efficiency [1–8]. Recently, Peled et al. [9,10] reported that methanol/oxygen and ethylene glycol/oxygen fuel cells equipped with a new nanoporous proton-conducting membrane and using PtRu/C (Pt:Ru atomic ratio of 1:1) as anode catalyst provided a maximum power density of 400 and 300 mW cm⁻², respectively, which puts ethylene glycol in direct competition with methanol as a promising candidate for practical electric vehicles and stationary applications.

Kelaidopoulou et al. [11] observed that the addition of ruthenium, tin or both onto platinum dispersed in poly-aniline (PANI) increases the electro-oxidation of ethylene glycol in acid medium. The PANI/Pt–Sn assembly showed the highest electro catalytic activity of the electrodes studied, however, the influence of PtSn composition was not investigated. We recently reported the electro-oxidation of ethylene glycol on PtRu/C and PtSn/C electrocatalysts with Pt:X (X = Ru or Sn) atomic ratios of 3:1, 1:1 and 1:3. Independent of the Pt:X atomic ratio used, PtSn/C electrocatalysts were better for ethylene glycol oxidation than PtRu/C electrocatalysts because the oxidation starts at lower potentials and high current values were obtained in the potential range for direct alcohol fuel cells (0.2–0.6 V) [12].

Table 1
Pt:Sn and Pt:Sn:Ni atomic ratios and mean particle size of the prepared electrocatalysts

Electrocatalyst	Nominal atomic ratio			Atomic ratio-EDX			Particle size ^a (nm)
	Pt	Sn	Ni	Pt	Sn	Ni	
PtSn/C	50	50	–	52	48	–	2.0
PtSnNi/C	50	40	10	52	42	6	2.4

^a Mean particle size calculated from X-ray diffraction data using the Debye–Scherrer equation.

* Corresponding authors. Tel.: +55 11 3133 9284.

E-mail addresses: espinace@ipen.br (E.V. Spinacé), aolivei@ipen.br (A.O. Neto).

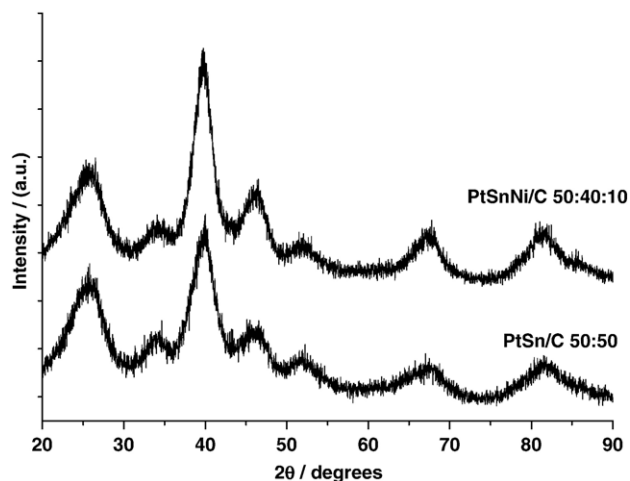


Fig. 1. X-ray diffractograms of PtSn/C and PtSnNi/C electrocatalysts.

In this work, PtSn/C electrocatalyst with Pt:Sn atomic ratio of 50:50 and a new formulation of PtSnNi/C electrocatalyst with a Pt:Sn:Ni atomic ratio of 50:40:10 were prepared by alcohol-reduction process [13,14] and tested for ethylene glycol oxidation using cyclic voltammetry and chronoamperometry.

2. Experimental

PtSn/C and PtSnNi/C electrocatalysts were prepared using $\text{H}_2\text{PtCl}_6 \cdot 6\text{H}_2\text{O}$ (Aldrich), $\text{NiCl}_2 \cdot 6\text{H}_2\text{O}$ (Aldrich) and $\text{SnCl}_2 \cdot 2\text{H}_2\text{O}$ (Aldrich) as metal sources, ethylene glycol (Merck) as solvent and reducing agent and Carbon Vulcan XC72R as support [13,14].

The Pt:Sn and Pt:Sn:Ni atomic ratios were obtained by EDAX analysis using a scanning electron microscope Philips XL30 with a 20 keV electron beam and provided with EDAX DX-4 microanalyser.

The XRD analyses were performed using a Rigaku diffractometer model Multiflex with a $\text{CuK}\alpha$ radiation source.

Transmission electron microscopy (TEM) was carried out using a Carl Zeiss CEM 902 apparatus with a Proscan high-speed slow-scan CCD camera and digitalized (1024×1024 pixels, 8 bits) using the AnalySis software. The particle size distributions were determined by measuring the nanoparticles from micrographs using Image Tool Software.

Electrochemical studies of the electrocatalysts were carried out using the thin porous coating technique [15,16]. An amount of 20 mg of the electrocatalyst was added to a solution of 50 mL of water containing 3 drops of 6% polytetrafluoroethylene (PTFE) suspension. The resulting mixture was treated in an ultrasound bath for 10 min, filtered and transferred to the cavity (0.30 mm deep and 0.36 cm² area) of the working electrode. The quantity of electrocatalyst in the working electrode was determined with a precision of 0.0001 g. In cyclic voltammetry and chronoamperometry experiments the current values (I) were expressed in amperes and were normalized per gram of platinum ($\text{A g}_{\text{Pt}}^{-1}$). The quantity of platinum was calculated considering the mass of the electrocatalyst present in the working electrode multiplied by its percentage of platinum. The reference electrode was a RHE and the counter electrode was a platinized Pt plate. Electrochemical measurements were made using a Microquimica (model MQPG01, Brazil) potentiostat/galvanostat coupled to a personal computer and using the Microquimica software. Cyclic Voltammetry was performed in a 0.5 mol L⁻¹ H_2SO_4 solution saturated with N_2 . The evaluation

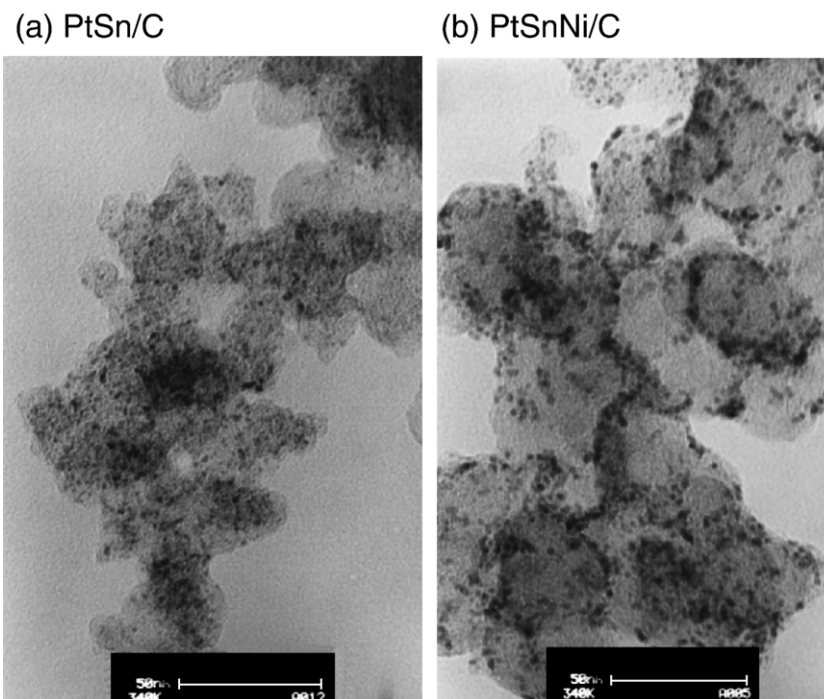


Fig. 2. Transmission electron micrographs of PtSn/C (a) and PtSnNi/C (b) electrocatalysts.

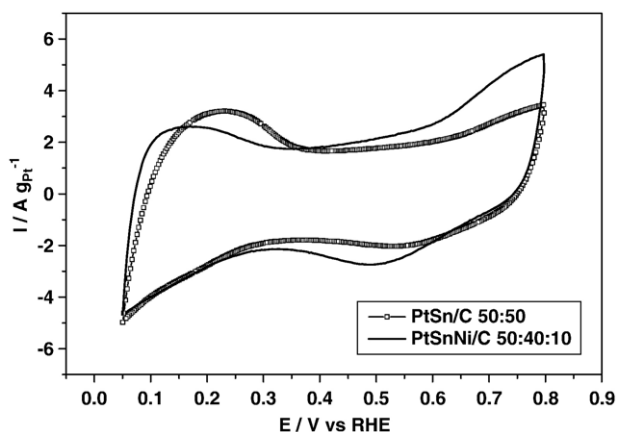


Fig. 3. Cyclic voltammograms of PtSn/C and PtSnNi/C electrocatalysts in $0.5 \text{ mol L}^{-1} \text{ H}_2\text{SO}_4$ with a sweep rate of 10 mV s^{-1} .

of ethylene glycol oxidation was performed at 25°C in three different concentrations: 0.1 , 0.5 and 1.0 mol L^{-1} . For chronoamperometry, the electrolyte solution was 1 mol L^{-1} of ethylene glycol in $0.5 \text{ mol L}^{-1} \text{ H}_2\text{SO}_4$.

3. Results and discussion

The carbon-supported PtSn/C and PtSnNi/C nanoparticles were prepared in a single step (co-reduction of mixed ions) using ethylene glycol as solvent and reducing agent in the presence of carbon Vulcan XC72R [12–14]. The Pt:Sn and Pt:Sn:Ni atomic ratios of the obtained electrocatalysts were similar to the nominal atomic ratios and the mean particle sizes were in the range of 2.0 – 2.5 nm (Table 1). The X-ray diffractograms of the electrocatalysts are shown in Fig. 1. The PtSn/C electrocatalyst showed four diffraction peaks at about $2\theta = 40$, 47 , 67 and 82° characteristic of the fcc structure of platinum and platinum alloys [16]. The broad peak at about 25° was associated with the Vulcan XC 72 R support material. It was also observed on the diffractogram two other peaks at about $2\theta = 34$ and 52° that were characteristic of cassiterite SnO_2 phase [17].

Xin and co-workers [18,19] prepared PtSn/C electrocatalysts by a similar procedure using ethylene glycol as reducing agent. The analysis of the diffractograms also revealed the typical peaks relative to the fcc structure of platinum alloy, however, no peaks of cassiterite phase were observed. This is probably because the electrocatalysts were prepared under argon flow while in this work the electrocatalysts were prepared in open atmosphere. The diffractogram of PtSnNi/C electrocatalyst also shows the characteristic peaks of the platinum fcc structure and the presence of cassiterite phase like observed for PtSn/C electrocatalyst.

TEM micrographs of PtSn/C (Fig. 2a) and PtSnNi/C (Fig. 2b) electrocatalysts showed a good distribution of the Pt particles on the carbon support with particle sizes of $2.0 \pm 1.0 \text{ nm}$, which is in agreement with XRD results.

The cyclic voltammograms (CV) of PtSn/C and PtSnNi/C electrocatalysts in the absence of ethylene glycol are shown in Fig. 3. In this case, all CV do not have a well-defined hydrogen adsorption–desorption region (0.05 – 0.4 V), which are characteristic of platinum alloys [20–22]. The CV of PtSnNi/C electrocatalyst showed higher currents values in the double layer region (0.4 – 0.8 V) than the PtSn/C electrocatalyst ($50:50$), which is probably due to the presence of tin and nickel oxide species [20–22]. In analysis of cathodic scan observe the reduction of oxides of nickel and tin in the potential $\approx 0.5 \text{ V}$. Sung and co-workers [23,24] prepared non-supported PtRu ($50:50$) and PtRuNi ($50:40:10$) nanoparticles prepared by a conventional reduction with NaBH_4 . The XRD analysis showed the characteristic peaks of platinum fcc structure and no peaks of fcc nickel and hcp ruthenium metals or oxides/hydroxides were observed. However, the XPS analysis revealed that about 40% of the ruthenium species were founded as ruthenium oxides and 85% of nickel species were founded as NiO , Ni(OH)_2 and NiOOH [23,24].

The PtSn/C and PtSnNi/C electrocatalysts performances in 1.0 mol L^{-1} of ethylene glycol oxidation are shown in Fig. 4. The cyclic voltammetry responses were normalized per gram of platinum, considering that ethylene glycol adsorption and dehydrogenation occur only on platinum sites at ambient temperature [25–28]. The electro-oxidation of ethylene glycol started at approximately 0.35 V for PtSn/C electrocatalysts while the substitution of a small amount of tin by nickel on the PtSnNi/C electrocatalyst decreased the onset potential to approximately 0.30 V and increased the current values in all range of the potential (Fig. 4). In Fig. 4 the currents values in the hydrogen region (0.05 – 0.4) decrease for 1.0 mol L^{-1} of ethylene glycol in relation cyclic voltammogram in absence of ethylene

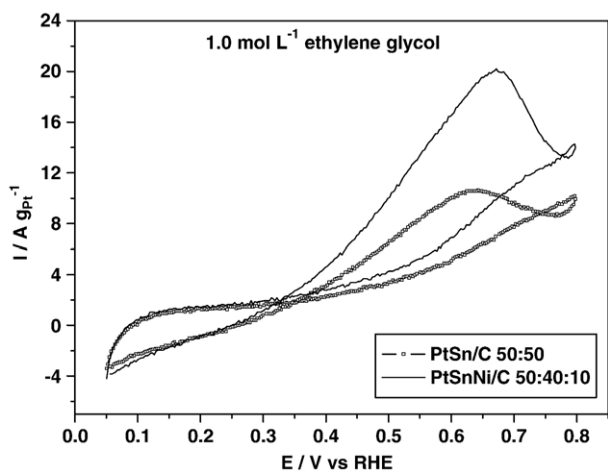


Fig. 4. Cyclic voltammograms of PtSn/C and PtSnNi/C electrocatalysts in $0.5 \text{ mol L}^{-1} \text{ H}_2\text{SO}_4$ containing 1.0 mol L^{-1} of ethylene glycol with a sweep rate of 10 mV s^{-1} .

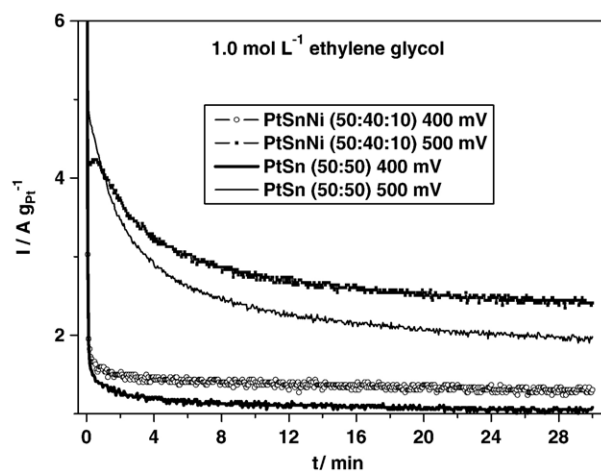


Fig. 5. Current–time curves at 0.4 and 0.5 V in 1 mol L^{-1} ethylene glycol solution in $0.5 \text{ mol L}^{-1} \text{ H}_2\text{SO}_4$ for PtSn/C $50:50$ and PtSnNi/C $50:40:10$ electrocatalysts.

glycol, most likely due to the adsorption of ethylene glycol on the nanoparticles surface, being able to cause the partial deactivation of the electrocatalysts.

The superior performance of the PtSnNi/C electrocatalyst was also confirmed by chronoamperometry measurements (Fig. 5). In all current–time curves there is an initial current drop in the first 5 min followed by a slower decay, but the current values obtained for PtSnNi/C electrocatalyst were always higher than those obtained for PtSn/C (50:50) electrocatalyst. Similar results were also observed in methanol oxidation using non-supported PtRu (50:50) and PtRuNi (50:40:10) electrocatalysts [23,24]. The superior activity of the PtRuNi electrocatalyst was attributed to the modification of electronic properties of platinum and to the presence of nickel oxide species resulting in a combination of electronic effect and bifunctional mechanism [23,24]. Recently, Dumesic and co-workers [29] reported the aqueous-phase reforming of oxygenated hydrocarbons, like glycerol and ethylene glycol, at temperatures near 500 K using non-precious metal catalysts. They observed that the addition of Sn to Raney–Ni catalysts facilitated C–C bond cleavage and promoted removal of adsorbed CO species by water–gas shift reaction, which increased the selectivity for hydrogen production.

4. Conclusions

The alcohol-reduction process was found to be an effective method for making active PtSn/C and PtSnNi/C (50:40:10) electrocatalysts for ethylene glycol oxidation. The X-ray diffractograms of electrocatalysts showed the typical fcc structure of platinum and platinum alloys with the presence of a cassiterite SnO₂ phase. PtSnNi/C electrocatalyst showed higher current values and stability than PtSn/C electrocatalyst in the potential range of interest for direct ethylene glycol fuel cell (0.30–0.60 V). Further work is however necessary to know if this is the optimum Pt:Sn:Ni composition and to conduct tests of these electrocatalysts in a single direct ethylene glycol fuel cell.

Acknowledgments

The authors thank Fundação de Amparo à Pesquisa do Estado de São Paulo — FAPESP and Conselho Nacional de Desenvolvimento Científico e Tecnológico-CNPq for financial support.

References

- [1] E.R. Gonzalez, *Quim. Nova* 23 (2000) 262.
- [2] H. Wendt, M. Linardi, E.M. Arico, *Quim Nova* 25 (2002) 470.
- [3] H. Wendt, M. Götz, M. Linardi, *Quim. Nova* 23 (2000) 538.
- [4] E.V. Spinacé, A. Oliveira Neto, E.G. Franco, M. Linardi, E.R. Gonzalez, *Quim. Nova* 27 (2004) 648.
- [5] L. Carrette, K.A. Friedrich, U. Stimming, *Fuel Cells* 1 (2001) 5.
- [6] B.C.H. Steele, A. Heinzel, *Nature* 414 (2001) 345.
- [7] C. Lamy, E.M. Belgsir, J.-M. Léger, *J. Appl. Electrochem.* 31 (2001) 799.
- [8] T. Iwasita, *Electrochim. Acta* 47 (2002) 3663.
- [9] E. Peled, T. Duvdevani, A. Ahron, A. Melman, *Electrochem. Solid-State Lett.* 4 (2001) A38.
- [10] E. Peled, V. Livshits, T. Duvdevani, *J. Power Sources* 106 (2002) 245.
- [11] A. Kelaidopoulou, E. Abelidou, A. Papoutsis, E.K. Polychroniadis, G. Kokkinidis, *J. Appl. Electrochem.* 28 (1998) 1101.
- [12] A.O. Neto, T.R.R. Vasconcelos, R.W.R.V. da Silva, M. Linardi, E.V. Spinacé, *J. Appl. Electrochem.* 35 (2005) 193.
- [13] E.V. Spinacé, A.O. Neto, T.R.R. Vasconcelos, M. Linardi, *Brazilian Patent BR200303471-A*.
- [14] E.V. Spinacé, A.O. Neto, T.R.R. Vasconcelos, M. Linardi, *J. Power Sources*, 137 (2004) 17.
- [15] A. Oliveira Neto, M.J. Giz, J. Perez, E.A. Ticianelli, E.R. Gonzalez, *J. Electrochem. Soc.* 149 (2002) A272.
- [16] F. Colmati Jr., W.H. Lizcano-Valbuena, G.A. Camara, E.A. Ticianelli, E.R. Gonzalez, *J. Braz. Chem. Soc.* 13 (2002) 474.
- [17] W.S. Cardoso, M.S.P. Francisco, A.M.S. Lucho, Y. Gushiken, *Solid State Ionics* 167 (2004) 165.
- [18] W. Zhou, Z. Zhou, S. Song, W. Li, G. Sun, P. Tsiakaras, Q. Xin, *Appl. Catal., B Environ.* 46 (2003) 273.
- [19] L. Jiang, G. Sun, Z. Zhou, W. Zhou, Q. Xin, *Catal. Today* 93–95 (2004) 665.
- [20] R.B. Lima, V. Paganin, T. Iwasita, W. Vielstich, *Electrochim. Acta* 49 (2003) 85.
- [21] E.V. Spinacé, A.O. Neto, M. Linardi, *J. Power Sources* 124 (2003) 426.
- [22] E.V. Spinacé, A.O. Neto, M. Linardi, *J. Power Sources* 129 (2004) 121.
- [23] J.-H. Choi, K.-W. Park, B.-K. Kwon, Y.-E. Sung, *J. Electrochem. Soc.* 150 (2003) A973.
- [24] K.-W. Park, J.-H. Choi, B.-K. Kwon, S.-A. Lee, Y.-E. Sung, H.-Y. Ha, S.-A. Hong, H. Kim, A. Wieckowski, *J. Phys. Chem., B* 106 (2002) 1869.
- [25] H.A. Gasteiger, N. Markovic, P.N. Ross, E.J. Carins, *J. Electrochem. Soc.* 141 (1994) 1795.
- [26] S.Lj. Gojkovic, T.R. Vidakovic, D.R. Durovic, *Electrochim. Acta* 48 (2003) 3607.
- [27] M. Christov, K. Sundmacher, *Surf. Sci.* 547 (2003) 1.
- [28] L. Dubau, F. Hahn, C. Countaceau, J.-M. Léger, C. Lamy, *J. Electroanal. Chem.* 554–555 (2003) 407.
- [29] G.W. Huber, J.W. Shabaker, J.A. Dumesic, *Science* 300 (2003) 2075.